Single- and double-wall flooding of two-phase flow in an annulus

W. A. Ragland
Reactor Analysis and Safety Division, Argonne National Laboratory, Argonne, IL 60439, USA

W. J. Minkowycz and D. M. France
Department of Mechanical Engineering, University of Illinois at Chicago, Chicago, IL 60608, USA

This study examined the phenomenon of flooding, defined as the transition from countercurrent to upward cocurrent flow, in an annular geometry. A total of 703 experimental determinations of the flooding point were made with water as the film and nitrogen as the upward-flowing gas. These data covered 10 configurations which varied with respect to physical location of gas and water inlets, number of wetted surfaces, and method of approach to flooding. Water flow rates were varied by a factor of 16 and gas flow rates by a factor of 4. The annulus dimensions were 90.64 mm inner diameter, 101.6 mm outer diameter, and 0.66 m long.

The widely used correlation of Wallis for tubes was applied to the annulus flooding data. The equation was found to predict the data satisfactorily with Wallis' original constants if the appropriate hydraulic diameters were used. These diameters were based upon visual observations of the flooding phenomenon, which occurred in two distinct modes.

Keywords: two-phase flow; flooding; annulus

Introduction

The flooding phenomenon may be generally described as the transition from countercurrent to cocurrent flow. The transition occurs when a liquid, initially flowing down under the influence of gravity, changes flow direction to coincide with the forced upward flow of a gas in the same channel. The phenomenon is important in many processes which rely on countercurrent flow to provide a highly active exchange interface for both heat and mass transfer.[1]

Specifically, flooding may be defined as the limit point at which any increase in either the liquid or gas flow rate results in less than all the liquid flowing downward. Several other definitions have also been used to describe flooding: (1) flooding occurs at the point that any of the liquid is in upward motion, even if the overall flow is downward; (2) flooding occurs when there is net flow reversal of the liquid; (3) flooding occurs at the onset of entrainment; and (4) flooding occurs when the liquid bridges the flow area. With all of these definitions of flooding, it is not surprising that the experimental observations of flooding yield systematic differences in the measurement of the flooding point. Further confusion arises from the converse situation of transition from upward cocurrent flow to countercurrent flow. This phenomenon is sometimes called deflooding and has been reported or analyzed as the condition for flooding.

A number of flooding studies have been conducted in cylindrical tubes, and the majority of the experiments involved diameters of 25 to 50 mm. Other parameters which have been studied include water inlet configuration, gas inlet configuration, flow channel length-to-diameter ratio, and phase change effects.

A major step in understanding the phenomenon of flooding came with the development of semiempirical predictive correlations which combined physical parameters with a limited number of empirical constants. The Wallis and Kutateladze correlations are widely used for cylindrical tube flow channels.

The approach used in the Wallis[2–4] correlation is to reduce the superficial velocity of both the gas and the liquid to their respective dimensionless velocities.

$$J_g^* = \rho_g^{1/2} j_g / [gD(\rho_l - \rho_g)]^{1/2} \tag{1}$$

and

$$J_l^* = \rho_l^{1/2} j_j / [gD(\rho_l - \rho_g)]^{1/2} \tag{2}$$

The dimensionless velocities are then combined in the form

$$J_g^{*1/2} + m J_l^{*1/2} = C \tag{3}$$

Based on cylindrical tube data, the values of the constants were found to be $0.88 \leq C \leq 1.0$ when $m = 1.0$.

Kutateladze[5] developed a correlation similar to the Wallis correlation. Wallis and Makkenchery[6] proposed that differences between the correlations due to surface tension effects could be expressed in terms of a dimensionless tube diameter by using the Bond number.

$$D^* = D[g(\rho_l - \rho_g)/\sigma]^{1/2} \tag{4}$$

For $D^* < 30$ the Wallis correlation was recommended, and for $D^* > 30$ the Kutateladze correlation was recommended. The Wallis correlation is appropriate for this study according to this criterion.

In recent years, more detailed correlations such as that of Richter, Wallis, and Speers[7] and Richter[8] have attempted to expand the original semiempirical correlations and provide additional physical basis. Dukler[9–11] investigated the statistical nature and the structure of large disturbance waves at a gas–liquid interface. Small ripples were studied by Chang and Dukler.[12] Maron and Dukler[13] and Dukler *et al.*[14] proposed a film model for flooding.

Address reprint requests to Dr. Minkowycz at the Department of Mechanical Engineering, University of Illinois at Chicago, Chicago, IL 60608, USA.

Received 10 May 1988; accepted for publication 6 September 1988

Experiment objectives

The general objective of this study was to investigate the flooding phenomenon in an annular geometry with liquid film established on both walls of the annulus as well as on each wall separately. The liquid flow rates on each wall were independently controlled to produce a wide range of flow conditions. The data from this investigation were compared to existing correlations to determine the various correlations' applicability to an annular geometry.

Two types of gas injection methods were studied: through-the-film and opposite-the-film for single-wall flooding. Single-wall flooding in this work was defined as flooding occurring from a countercurrent flow configuration in which the liquid film was present initially only on one wall of the annulus. The two water inlets and two gas inlets to the test section shown in Figure 1 provided four physical single wall flooding configurations. The single-wall flooding configuration with the liquid film on the outside wall and gas injection from the inside wall was expected to have the closest similarity to studies of flooding which have been performed in cylindrical tubes. The case with both liquid (water) and gas (nitrogen) on the inside wall was expected to simulate the fluid mechanics but not heat transfer portion of single-component, two-phase flooding in which the film is boiled off of a hot wall. A situation of this general type can occur during the emergency core cooling of a nuclear reactor, and the phenomenon is better represented by an annulus configuration than by flow inside of a circular tube. This study presents the first annulus flooding tests with liquid flow on both walls, and the boiling effect on the liquid film was included by using the inside wall gas injection to lift the smooth liquid film from the wall much in the manner that nucleate boiling from a surface may disrupt the film. The single-wall flooding experiments also included an investigation of the influence of the approach to flooding, i.e., varying the velocity of one fluid while maintaining constant the velocity of the other fluid.

Two-wall flooding, in this study, is defined as flooding occurring from a countercurrent flow configuration in which a liquid film is established initially on both walls of the annulus. Two configurations of two-wall flooding were investigated by using the two gas inlets shown in Figure 1. The primary objective of the two-wall flooding investigation was to vary the liquid velocities on each wall and to compare the results to the single-wall flooding data.

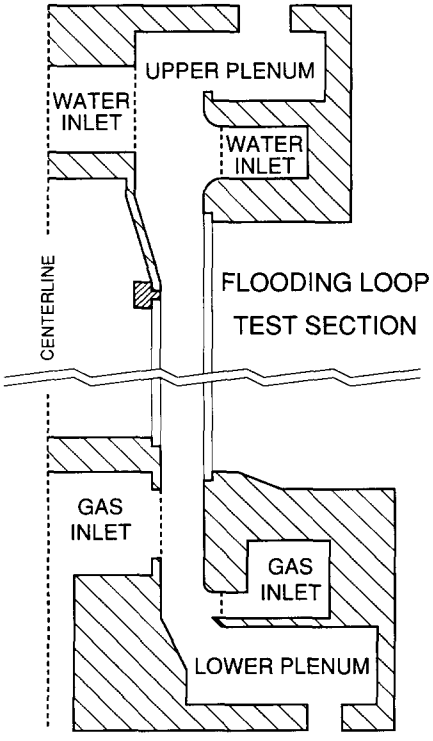

Figure 1 Test section

Test apparatus description

The primary piece of equipment used in this research was a flooding loop located at Argonne National Laboratory. Details of the loop are given by Ragland,[15] and a schematic of the annulus test section is shown in Figure 1. The four fluid inlets to the test section were through porous material which provided uniform circumferential distribution. The porous material with its relatively large pressure drop produced flows that were uniform during an entire test duration. They also provided an inherent flow measurement, and they were calibrated for this purpose. Dukler *et al.*[14] and Maron *et al.*[16] both used the porous media inlet approach. The flow rates through each of the four inlets were independently controllable and were used to establish the different flow configurations of this study. These four inlets allowed the simulation of a boiling situation in the lower region of the test section, and gas was injected either through or opposite a liquid film. The liquid flow rate range was 0.007 to 0.173 l/s, which, in the test section of Figure 1, corresponded to superficial velocities of 0.01 to 0.11 m/s. The gas flow rate range was 4.1 to 17.5 l/s, corresponding to superficial velocities of 2.5 to 10.6 m/s. All tests were performed at approximately 1 atm and 27°C. The test section was made of glass to allow visual observations of the flooding phenomenon. The inner glass tube had an inner diameter of 101.6 mm and was 0.945 m long. The annular gap formed by the two tubes was 5.46 mm.

Notation

A	Flow area, m^2
C	Experimentally determined constant
D	Tube diameter, m
D^*	Bond number, defined by Equation 4
g	Acceleration of gravity, m/s^2
j	Superficial velocity, m/s
J^*	Dimensionless velocity defined by Wallis (Equations 1–2)
m	Experimentally determined constant
P	Perimeter, m
ρ	Density, g/m^3
σ	Surface tension, N/m

Subscripts

g	Gas
i	Annulus inner surface
l	Liquid
o	Annulus outer surface

Test procedure

The order of testing was as follows: (1) the single-wall flooding point was approached by increasing gas flow while maintaining a constant water flow; (2) the single-wall flooding point was approached by increasing water flow while maintaining a constant gas flow; and (3) the two-wall flooding point was approached by increasing gas flow after establishing a prescribed liquid film on each wall. The investigation of flooding with liquid on both walls was divided into two areas. One of these was a general investigation of the two-wall flooding, and the second was an investigation of flow-split effects on a constant total flow. The total flow for the flow-split flooding investigations was chosen to be equal to the maximum flow obtainable through the inner water inlet. This choice allowed the maximum variation in percentage of flow between the two walls. During each run, the flow rates of the liquid and gas and the differential pressure across the length of the annulus were recorded as functions of time on an FM analog tape recorder.

Experimental results

In the presentation of experimental flooding results, the data from all of the individual runs were grouped by physical flow configurations and method of approach to flooding as summarized in Table 1. The four single-wall flooding configurations with flooding approached by varying gas flow while maintaining constant liquid flow are listed as configurations 1–4. Configurations 11–14 are the configurations in which flooding was approached by increasing the water flow rate while maintaining a constant gas flow rate. The general two-wall flooding runs are divided into configurations 5 and 6 as a function of the gas inlet. The flow-split runs are designated configurations 15 and 16 and are also divided as a function of gas inlet.

Single-wall flooding

Configuration 1 runs approached flooding using a constant water flow through the outer water inlet while nitrogen flow was increased through the inner gas inlet. As the nitrogen flow approached the flooding point, a "bulge" occurred in the film on the outer wall slightly above the elevation of the top of the inner gas inlet. This bulge may have been similar to that investigated by Wallis and Makkenchery[6] or Shearer and Davidson.[17] This standing wave also served as an initiator of disturbance waves on the liquid surface. Visually, these disturbances could only be detected for 60 to 80 mm above the bulge and increased with gas flow similar to that reported by Meyer and Giot.[18] As the gas flow was increased to flooding, the liquid bridged the lower part of the test section and an immediate flow reversal followed. At the moment that the liquid bridged the entire annular gap, the test section pressure drop abruptly increased by a significant amount. The point of flooding was very clear. Pressure measurements for all tests are given by Ragland.[15]

Configuration 11 was the same as configuration 1 except that the gas flow remained constant while the water flow was increased. Gas and liquid flow rate data at the flooding points from 179 configuration 1 and 11 tests are shown in Figure 2. The approach to flooding is seen not to have influenced the results.

Configuration 2 tests were performed with gas entering the test section through the outer gas inlet and the water film on the test section outer wall. Gas passing through the film caused

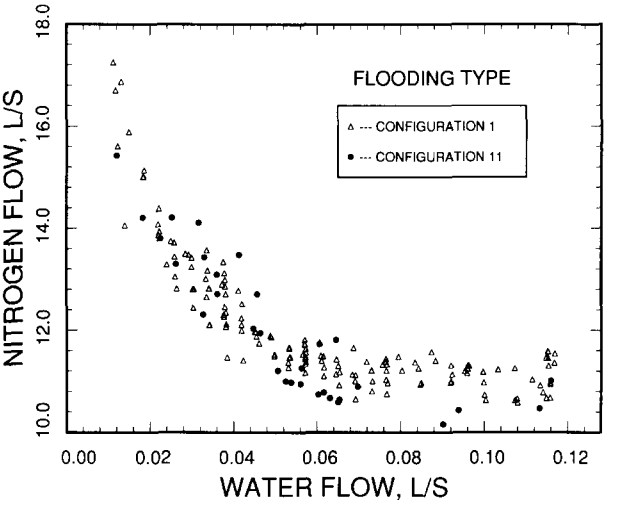

Figure 2 Outer-wall flooding without inlet interference

Table 1 Flood configurations

Type of run	Number of runs	Water: Inlet location In	Water: Inlet location Out	Water: Range Volume flow (l/s)	Water: Range Superficial velocity (m/s)	Gas: Inlet location In	Gas: Inlet location Out	Gas: Range Volume flow (l/s)	Gas: Range Superficial velocity (m/s)	Remarks
1	148		X	0.010–0.120	0.01–0.07	X		10.5–17.5	6.4–10.6	Steady water
2	88		X	0.007–0.117	0.01–0.07		X	5.7–13.6	3.5–8.3	Steady water
3	83	X		0.026–0.087	0.02–0.05		X	5.8–7.9	3.5–4.8	Steady water
4	82	X		0.040–0.090	0.02–0.05	X		7.2–9.7	4.4–5.5	Steady water
5	73	X	X	0.080–0.173	0.05–0.11		X	4.1–5.8	2.5–3.5	Two wall
6	50	X	X	0.080–0.170	0.05–0.11	X		5.7–7.6	3.5–4.6	Two wall
11	31		X	0.012–0.116	0.01–0.07	X		10.2–15.4	6.2–9.4	Steady gas
12	22		X	0.034–0.118	0.02–0.07		X	5.8–8.8	3.5–5.4	Steady gas
13	3	X		0.060–0.070	0.05		X	6.5	4.0	Steady gas
14	17	X		0.056–0.098	0.03–0.06	X		7.7–82.	4.7–5.0	Steady gas
15	53	X	X	0.098	0.06		X	4.9–6.0	3.0–4.6	Flow split
16	53	X	X	0.098	0.06			6.6–7.6	4.0–4.6	Flow split
Total 703				0.007–0.173	0.01–0.11			4.1–17.5	2.5–10.6	

disruption of the film and liquid entrainment at lower gas velocities than in configuration 1 tests. This condition in configurations 2 and 12 was observed as a type of churned flow in the lower part of the test section prior to flooding. The test section differential pressure rose to a higher level and was much "noisier" prior to flooding as compared to configurations 1 and 22. The pressure response was an indication of the more chaotic nature of the test section flow.

The flooding data for configurations 2 and 12 exhibited trends similar to the configuration 1 and 11 results of Figure 2. The approach to flooding, by varying gas or liquid flow rate, did not influence the test results. However, the effect of the flow churning was to lower the flooding gas flow; i.e., the annulus flooded more easily at a given liquid flow rate for configurations 2 and 12 compared to configurations 1 and 22.

Configuration 3 and 4 tests were conducted with water at a constant flow entering the inner water inlet to the test section. Nitrogen gas flow was increased through the outer gas inlet in configuration 3 and through the liquid film in configuration 4. The lower limit of water flow rate for these tests was controlled by film breakdown on the inner wall of the test section. Film breakdown typically began at a location where a metal connecting ring, shown crosshatched in Figure 1, joined the inner glass tube to the Plexiglas cone used to spread the flow above the test section. As will be shown later, this surface imperfection or discontinuity may also have contributed to a break in the flooding curve for extremely low water flow rates.

Flooding in configuration 3 and 4 runs occurred in one of two modes. The most common mode commenced when a churned, two-phase mixture formed in the lower part of the test section and gradually increased in height with some surging until the entire test section was filled with the two-phase mixture. At this point, fluid began to build up in the liquid entrance to the test section, and the test section pressure drop increased substantially, as occurred with all flooding tests. This mode of flooding was designated as climbing flooding. The other mode of flooding occurred when the incoming liquid flow suddenly built up above the test section in the entrance region resulting in a rather chaotic flow throughout the entire test section. This mode of flooding was designated as top flooding. Most of the climbing flooding occurred at an inner water flow rate greater than 0.05 l/s. The top flooding runs all occurred at water flow rates below 0.06 l/s. The configuration 4 flooding data of Figure 3 show a sharp break in the gas flow required for flooding occurring at an inner water flow rate which is approximately the upper limit for top flooding. The configuration 3 results were similar to Figure 3.

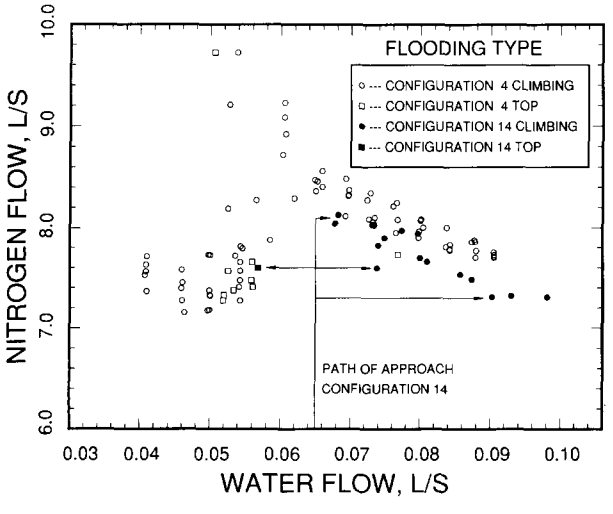

Figure 3 Inner-wall flooding with inlet interference

In a significant proportion of runs at low water flow rates, very large drops of water were observed being violently entrained from the film on the inner wall at the location of the metal support ring at the top of the test section or at the point where the conical flow expander curves to form the annulus. These large drops were propelled across to the outer wall of the annulus. The magnitude of flow transferred from the inner wall to the outer wall varied from a few drops usually at lower gas velocities to sufficient flow to cause at least partial wetting of the outer wall forming rivulets and sometimes sheets of water on the outer wall. This phenomenon is not considered to be of a general nature, but rather it appears to be related to the surface discontinuity and change in shape in the test section of this study. However, these anomalies in the test section provided a mechanism for transfer of liquid to the outer wall, and when this transfer was significant the system behaved just as one would expect from the results of the two-wall flooding tests. The later results will be discussed subsequently. Thus, only the higher water flow rate data of Figure 3 (above 0.06 l/s) can be attributed to single-wall flooding. The general trend of those data are similar to the data of configurations 1, 2, 11, and 12.

Flooding was approached in configurations 13 and 14 by varying the water flow rate at constant gas flow rate. Seventeen configuration 14 results are shown in Figure 3. Sixteen of these correspond to flooding approached by increasing the liquid flow rate. The results, shown in Figure 3 as solid circles, indicate no significant difference from the variable gas flow tests of configuration 4. The remaining 17th run approached flooding in an unusual manner, by decreasing the water flow rate at a constant gas velocity. In this case, flooding occurred at the top flood mechanism. Approaching flooding by decreasing the water flow rate provided verification of the bimodal or multi-valued behavior of the configuration 14 data with respect to water flow rate.

Two-wall flooding

Two-wall flooding experiments were conducted with a liquid film on both walls of the annulus. The tests are denoted as configuration 5 or 6, depending on the gas inlet used as given in Table 1. The results shown in Figure 4 are similar for both configurations. Most of the data represent climbing-type flooding, and top flooding occurred only at the lowest liquid flow rate. The trend of the flooding point data is not as definite for this two-wall case compared with single-wall flooding results.

The effect of the division of flow between outer and inner wall films in two-wall flooding was investigated further in configurations 15 and 16. In both configurations, the total liquid flow was a constant for all tests. The percentage of flow varied among tests, and the two configurations were distinguished by the gas inlet used as given in Table 1. Results from configuration 15 runs are shown in Figure 5. The fraction of water flow on the inner wall was varied from 25 to 85% of the total flow. These two-wall flooding data of Figure 5 were enhanced by adding single-wall data at the same total flow rate from configurations 2 and 3. This procedure effectively extrapolated the two-wall flooding data to the limits of 0 and 100% liquid flow on each wall. Taken together, the data of Figure 5 indicate a minimum in the gas flooding flow rate occurring when the liquid flow is split approximately evenly between the two walls. The configuration 16 data exhibit similar trends.

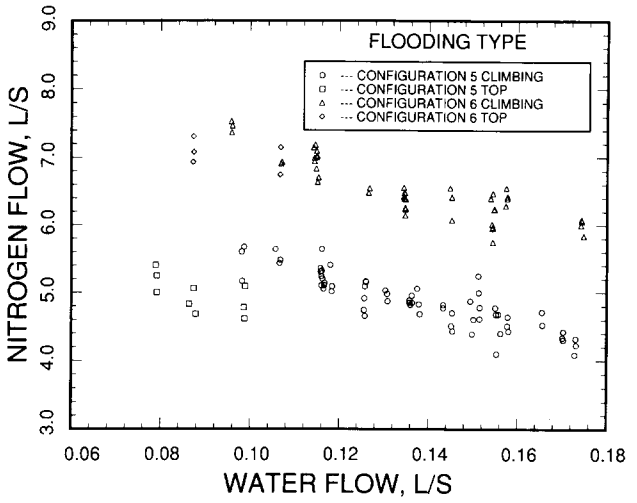

Figure 4 Two-wall flooding

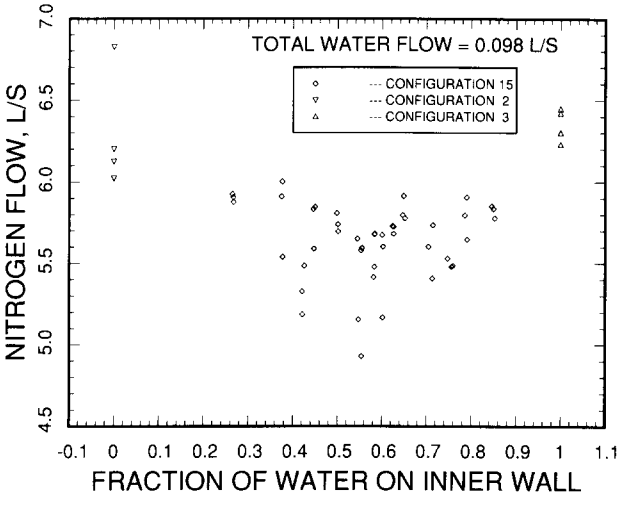

Figure 5 Two-wall flooding with constant total flow

Discussion

Single-wall flooding mechanisms

The nature of the flow at flooding in configurations 1 and 11 was observed to be significantly different from the six other single-wall flooding configurations, 2–4 and 12–14. Correspondingly, the flooding data exhibited a clear distinction as seen in Figure 6. Notwithstanding the various geometry factors of the two sets of inlets, configurations 1 and 11 data, with gas from the inner wall inlet and water from the outer wall inlet, produced a flooding behavior in which the gas flooding flow rate was approximately 40% greater than in the other configurations at a given liquid film flow rate. Visual observation of the mechanism of flooding for configurations 1 and 11 can best be described as an abrupt or catastrophic change of flow pattern in which two separated streams of countercurrent flow lost their interfacial integrity. The resulting flow pattern was one of virtually total upward cocurrent flow. This abrupt change of flow pattern is contrasted with that for all of the other configurations in which a clear interface between gas and liquid did not exist as the point of flow reversal was approached. Early bridging occurred in the majority of these test cases, and the two-phase region began to grow upward with increasing gas flow with varying amounts of surging or chugging. The surging and chugging increased as did the extent of the two-phase region until eventually it moved upward throughout the entire length of the test section. The final resultant flow configuration was one of mixed flow in which some of the fluid still managed to penetrate to the lower plenum, but a portion of the fluid was held up above the test section and unable to enter.

Two-wall flooding

Trends in the two-wall flooding data were considered with respect to either the outer water flow rates or the inner water flow rate, separately. It was found that the governing flow rate is the total water flow rate rather than either the inner or outer water flow rates. In addition to these data, visual observations of the test section, during two-wall flooding with a very thin film on the inner wall, showed the same mechanism of transfer of liquid from the inner to the outer wall to be operating as was seen in some of the single-wall cases with the thin film on the inner wall. Since the outer wall was already wet, however, this transfer of liquid did not cause an abrupt break in the data as in the single-wall flooding cases. Further insight concerning the effect of the water transfer was gained by comparing two-wall and single-wall flooding results.

Two-wall versus single-wall flooding

Two-wall flooding was compared to single-wall flooding in Figure 5 using two flow-split data of configuration 15. A minimum in the gas flow rate was noted when the liquid film was evenly divided on the two annulus walls. Chang and Dukler[12] suggested that the main contribution to interfacial friction was the presence of small ripples on the surface of the liquid. Richter[8] used interfacial friction related through a friction factor[4] for wavy annular flow. Both of these approaches related the waviness of the film, through an interfacial friction factor, to the gas pressure drop. Since interfacial friction also represents a means of energy transfer from gas to liquid, its energy could serve to form additional waves. Such a mechanism could be taking place constantly above the churned turbulent region of the test section. Thus, the test section could be divided into two parts, the lower part being the churned turbulent

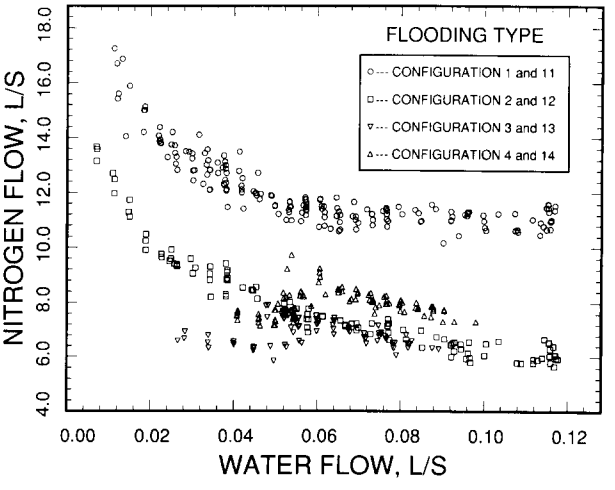

Figure 6 Bridged and unbridged flooding

region in which the gas is attempting to lift fluid which is already bridged, and the upper region in which the interaction of gas and liquid film on the wall may cause further bridging. It is consistent with this reasoning that if all of the fluid is on one wall, there would be no energy transfer from gas to liquid on the other wall, and with the transfer area reduced in half the flooding rate would be expected to be higher. The gas flow rate at flooding was generally higher for single-wall than two-wall flooding at the same liquid flow rate. The minimum gas flow rate occurring at equal film flow rates in two-wall flooding can be explained by further comparison of results with the single-wall case.

The single-wall flooding results without wall-to-wall liquid transfer effects are shown in Figures 2 and 6. The gas flow rate at flooding is most sensitive to film flow rate in the lower range of liquid film flow rate. Thus, the major change in reducing the gas flow rate on the flooding curve occurs as the liquid film first begins to thicken, but the rate of change decreases asymptotically. Based on this observation, the 50% flow split appears most likely to produce a minimum gas flow rate at flooding. A change from this split would cause one film to suffer a decrease in flow rate. That film alone would require an increased gas flow rate to flood, while the thickened film alone would flood at a lower gas flow rate. Due to the nonlinearity of the data trend of Figures 2 and 6, the magnitude of the gas flow rate at flooding is more sensitive to the thin-film requirement. Consequently, the gas flow rate for two-wall flooding should increase on a flow-split deviation from 50% toward either 0% or 100%. This condition was observed experimentally, as seen in Figure 5.

Data from single-wall flooding configurations 3 and 4 resembled two-wall flooding at low liquid flow rates. It was observed that liquid was present on both walls at the flooding point, and the data trend changed significantly as previously discussed. The single-wall flooding results from configuration 3 were compared with two-wall flooding data of configuration 5. The results shown in Figure 7 clearly indicate that the low-film-flow single-wall flooding data are an extension of the two-wall flooding data. At low film flow rates in single-wall tests, the liquid transferred to the outer wall in effect created a form of two-wall flooding. This result is clear in the data even though the transferred liquid did not appear to form a complete film. Therefore, what could have been considered an anomaly in the configuration 3 data (i.e., a break in the flooding curve) is in effect a subset of data that should be classified as two-wall flooding.

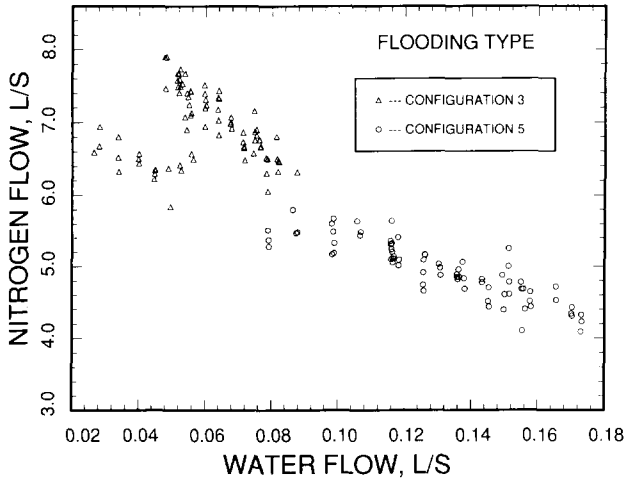

Figure 7 Two-wall flooding in single-wall tests

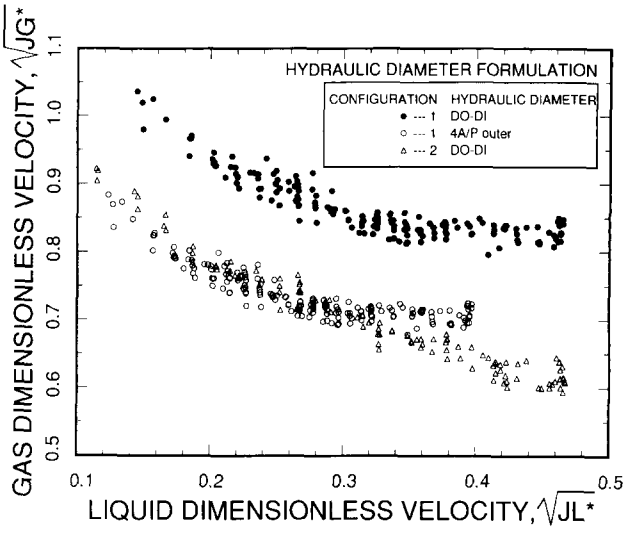

Figure 8 Effect of hydraulic diameter form

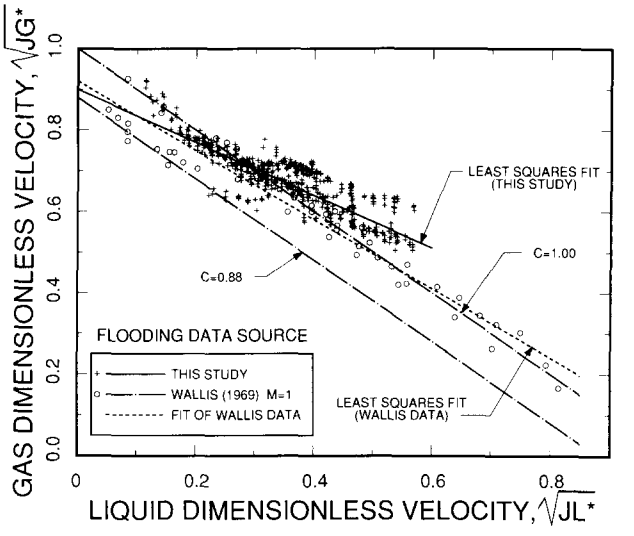

Figure 9 Correlation of data

Comparison with predictions

The Wallis correlation[2-4] for flooding in round tubes was applied to the annulus data of this study. It was necessary to choose a characteristic dimension to replace the diameter in the Wallis correlation, and the choice was not obvious, due to the dependence of the flooding phenomenon on the character of the liquid-gas interface. Simply using the hydraulic diameter in the usual manner would not be expected to apply in all cases. For example, flooding with a single film on the outer wall would be expected to be influenced by the inner wall diameter in a small secondary way through a change in the gas velocity profile. The hydraulic diameter, which is sensitive to the inner wall diameter, would be inappropriate for use as a characteristic dimension in this situation. However, it was possible to obtain a satisfactory fit of the Wallis correlation to the annulus data provided the hydraulic diameter was correctly formulated. The hydraulic diameter was based on the area of the annulus and the liquid wetted perimeters prior to flooding. The first type of flooding, observed for configurations 1 and 11 where the two

fluid streams were separate until the time of flooding, was characterized by a wetted perimeter equal to the outer circumference of the annulus. The second type of flooding, involving all of the other configurations, was characterized by the normal hydraulic diameter where the wetted perimeter was the sum of the inner and outer circumferences of the annulus.

Results are shown in Figure 8 for the dimensionless velocities of the Wallis correlation. Configuration 1 data are seen to be superimposed on configuration 2 data if the hydraulic diameters are chosen as discussed.

Using these different hydraulic diameters for the two types of flooding observed, all of the data of this study (703 tests) were compared to the Wallis correlation in Figure 9. The bounds of the correlation for the parameters $C=0.88$ and $C=1.00$ are shown. The prediction of the upper bound of the correlation was reasonable compared to the data and to least squares curve fits to the data. Keeping the constant, $m=1$, in the Wallis correlation resulted in a best fit value of $C=1.03$, which compared favorably to the Wallis upper limit of $C=1.00$. A slightly better curve fit to the data of this study was obtained by optimizing both parameters m and c. The result, shown in Figure 9, is $m=0.65$ and $c=0.90$.

A portion of Wallis' data [4] is shown in Figure 9. In the range of liquid velocities of this study, the Wallis data have approximately the same slope and fall just below the present data. The curve fit to all of the Wallis data with deflooding data removed as shown in Figure 9 is closer in slope to the data of this study than the Wallis correlation, although the difference is not large. In general, the comparisons of Figure 9 indicate reasonably good agreement between annulus data, tube data, and tube correlation if the appropriate hydraulic diameters are used.

Conclusions

Two general types of flooding were observed in all of the configurations tested in the annular geometry. These types were distinguished by whether or not liquid bridged the annular gap prior to flooding. Bridging did not occur in configuration 1 and 11 tests, in which case the test section flooded from a surface instability. The gas velocity at flooding was found to be aproximately 40% higher for flooding in the nonbridged cases than in the bridged cases. Bridging and churning flow near the bottom of the test section occurred in all tests where the gas entered the annulus through a liquid film. In addition, bridging occurred in configurations 3 and 13 as a consequence of the gas inlet geometry.

The approach to flooding, using variable liquid or variable gas flow was found to have no measurable effect on flooding conditions. However, the distribution of liquid flow on the walls of the annulus had a significant effect. Minimum gas flow rates at flooding occurred when the liquid flow rate was evenly split between the two walls. It was maximum in the condition of single-wall flooding, although low-liquid-flow single-wall flooding from the inner wall was found to resemble two-wall flooding as a consequence of liquid transfer to the outer wall.

All of the annulus data, including both types of flooding and single-wall and double-wall configurations, were successfully correlated with the Wallis correlation for round tubes using appropriate hydraulic diameters. Wallis' parameters of $m=1$ and $c=1$ predict the annulus flooding data reasonably well. Constants of $m=0.65$ and $c=0.90$ fit the annulus data the best and are recommended in the range of these data, $0J_g^*<0.57$.

Application of the data of this study to engineering design situations requires some consideration of conservatism. In all of the configurations tested in a controlled laboratory environment, only configurations 1 and 11 produced high gas flow rate flooding which occurred from an unbridged condition. Several factors were shown to cause bridging in the other configurations. A conservative approach to flooding prediction would be to assume that bridging will always occur in the annulus unless there is specific evidence to the contrary. (This conservative assumption applies to configurations 1 and 11 as well as the others.) This approach is equivalent to using the normal hydraulic diameter for the annulus with the correlation equations presented.

References

1 Cheremissinoff, N. P. and Cheremisinoff, P. N. Countercurrent flow through fixed-bed reactors. In *Handbook of Fluids in Motion*, eds. Cheremisinoff and Gupta, 1983, pp. 561–581

2 Wallis, Graham B. Annular two-phase flow: Part 1. A simple theory. *ASME J. Basic Engineering*, 1970, **92**, 59–72

3 Wallis, Graham B. Annular two-phase flow: Part 2. Additional effects. *ASME J. Basic Engineering*, 1970, **92**, 73–82

4 Wallis, Graham B. *One Dimensional Two-Phase Flow*, McGraw-Hill, New York, 1969

5 Kutateladze, S. S. Elements of the hydrodynamics of gas-liquid systems. *Fluid Mechanics—Soviet Research*, 1972, **4**, 29–103

6 Wallis, Graham B. and Makkenchery, S. The hanging film phenomenon in vertical annular two-phase flow. *J. Fluids Engineering*, 1974, **96**, 297–298

7 Richter, H. J., Wallis, G. B., and Spears, M. S. Effect of scale on two-phase counter current flow flooding. U.S. Nuclear Regulatory Commission, NUREG/CR-0312, 1979

8 Richter H. J. Flooding in tubes and annuli. *Int. J. Multiphase Flow*, 1981, **7**(6), 647–658

9 Telles, A. S. and Dukler, A. E. Statistical characteristics of thin, vertical, wavy, liquid films. *Ind. Eng. Chem. Fundam.*, 1970, **3**, 412–421

10 Chu, K. J. and Dukler, A. E. Statistical characteristics of thin, wavy films: Part II. Studies of the substrate and its wave structure. *A.I.Ch.E. J.*, 1974, **20**, 695–706

11 Chu, K. J. and Dukler, A. E. Statistical characteristics of thin, wavy films: Part II. Structure of the large waves and their resistance to gas flow. *A.I.Ch.E. J.*, **21**, 583–593

12 Chang, F. W. and Dukler, A. E. The influence of a wavy interface on pressure drop in conduits. *Int. J. Heat Mass Transfer*, 1964, **7**, 1395–1404

13 Maron, D. Moalem and Dukler, A. E. New concepts on the mechanisms of flooding and flow reversal phenomena. *Letters in Heat and Mass Transfer*, 1981, **8**, 453–463

14 Dukler, A. E., Smith, L., and Chopra, A. Flooding and upward film flow in vertical tubes: I. Experimental studies. *Int. J. Multiphase Flow*, 1984, **10**(5), 585–597

15 Ragland, W. A. A study of two-phase counter-current flow at the flooding point in an annular geometry. Ph.D. Thesis, University of Illinois at Chicago, Chicago, Ill.

16 Maron, D. Moalem and Dukler, A. E. Flooding and upward film flow in vertical tubes: II. Speculations on film flow mechanisms. *Int. J. Multiphase Flow*, 1974, **10**(5), 599–621

17 Shearer, C. J. and Davidson, J. F. The investigation of a standing wave due to gas blowing upwards over a liquid film; its relation to flooding in wall-wetted columns. *J. Fluid Mech.*, 1965, **22**, 321–335

18 Meyer, B. and Giot, M. Experiments and modeling of flooding phenomena. *Nuclear Engineering and Design*, 1987, **99**, 75–84